

Activated carbon supported nitrogen-containing diheterocycle mercury-free catalyst for acetylene hydrochlorination

Xingzong Dong^{a,b}, Guangye Liu^a, Zhaoan Chen^a, Quan Zhang^{a,b}, Yunpeng Xu^{a,*}, Zhongmin Liu^{a,b}

^a National Engineering Laboratory for Methanol to Olefins, Dalian National Laboratory for Clean Energy, Dalian Institute of Chemical Physics, Chinese Academy of Sciences, Dalian 116023, PR China

^b School of Chemical Engineering, University of Chinese Academy of Sciences, Beijing 100049, PR China

ARTICLE INFO

Keywords:

Acetylene hydrochlorination
Mercury free catalyst
Nonmetallic catalyst
Nitrogen-containing diheterocycle

ABSTRACT

An original nonmetallic mercury-free catalyst for the production of vinyl chloride monomer (VCM) by acetylene hydrochlorination was studied in this work. It was first found that a nitrogen-containing diheterocycle, 1,8-diazabicyclo[5.4.0]undec-7-ene hydrochloride ([DBU][Cl]), displayed excellent catalytic performance in acetylene hydrochlorination. The 20%[DBU][Cl]/AC catalyst exhibited an acetylene conversion of 86.7% and a selectivity to VCM of 99.2%, and the deactivation rate was only 0.033 %/h during the 200 h lifetime evaluation under the conditions of a bed temperature of 240 °C, GHSV(C₂H₂) of 30 h⁻¹ and V(HCl)/V(C₂H₂) of 1.2. TPD characterizations and intermittent flow experiments revealed that the 20%[DBU][Cl]/AC catalyst has a larger HCl adsorption capacity and smaller VCM adsorption capacity, which may be one of the reasons for the good catalytic activity and stability. The catalytic mechanism over [DBU][Cl] was proposed based on DFT calculations.

1. Introduction

Polyvinyl chloride(PVC) is one of the most important general plastic and has a wide range of applications, especially in the construction industry [1]. The production of PVC relies on the polymerization process of vinyl chloride monomer (VCM). At present, acetylene hydrochlorination is the main process for the production of VCM in coal-rich regions [2]. The activated carbon supported HgCl₂ (HgCl₂/AC) catalyst is used in the current industrial process of acetylene hydrochlorination process, which is highly toxic and prone to sublimation. These disadvantages result in mercuric chloride catalyst deactivation and environmental pollution problems simultaneously [3]. The Minamata Convention has been signed to ban the production and exchange of mercury products in the world. Hence, it is imperative to exploit an eco-friendly and low-cost catalyst as alternative to HgCl₂/AC in the production of VCM.

In 1985, Hutchings et al. conducted a preliminary investigation on the correlation between the initial catalytic activity of metal chlorides and the standard electrode potential [4]. This opened the prelude to the study of nonmercury catalysts for hydrochlorination of acetylene. In the past decades, researchers have mostly focused on the application of

different metal chlorides in the hydrochlorination of acetylene, such as AuCl₃ [1,4,5], K₂PtCl₄ [6–8], PdCl₂/K₂PdCl₄ [9,10], RuCl₃ [3,11–13], CuCl₂ [14,15] and BiCl₃ [16,17]. In recent years, researchers have conducted in-depth research on metal salt supported catalysts such as Na₃Au(S₂O₃)₂/AC [1], Au-SCN/AC [18], Ru-IL/AC [19] and Cu-1HEDP/AC [20] and developed a series of mercury-free catalysts with considerable application potential. Nevertheless, the commercialization of metal catalysts for acetylene hydrochlorination has been limited due to high cost, scarce mineral reserves and poor impurity tolerance.

The nonmetallic catalysts previously reported mainly include heteroatom-doped carbon [21–23], carbon nitride materials [24–26], boron nitride materials [27,28], graphene carbon [29,30] and defective carbon materials [31–33]. For example, Li et al. manufactured a SiC@N–C nanocomposite for acetylene hydrochlorination that displayed acetylene conversion over 80% and excellent VCM selectivity, and it was subjected to 150 h endurance test [24]. Li and coworkers prepared N, P-codoped carbon materials by the self-assembly method, which displayed excellent catalytic activity and resistance to high temperatures and impurities during a 400 h test [34]. Previous work has proven that the prominent HCl adsorption and activation ability makes

* Corresponding author.

E-mail address: xuyunpeng@dicp.ac.cn (Y. Xu).

<https://doi.org/10.1016/j.mcat.2022.112366>

Received 2 March 2022; Received in revised form 19 April 2022; Accepted 11 May 2022

Available online 19 May 2022

2468-8231/© 2022 Elsevier B.V. All rights reserved.

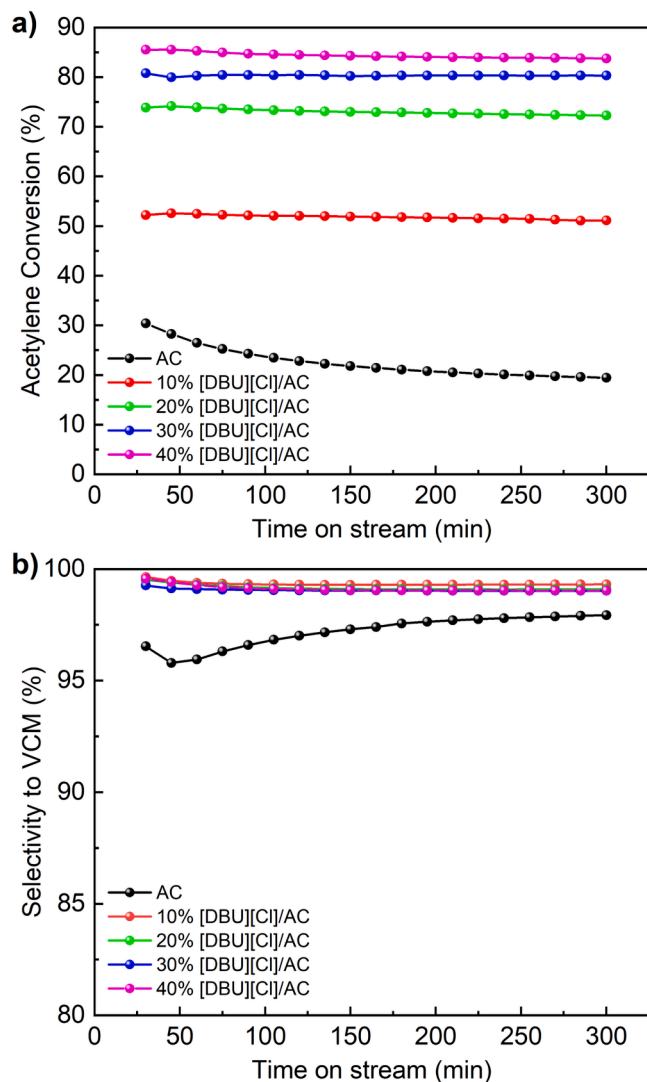


Fig. 1. Acetylene conversion (a) and selectivity to VCM (b) over the different catalysts. Reaction conditions: $T = 240\text{ }^{\circ}\text{C}$, $\text{GHSV}(\text{C}_2\text{H}_2) = 60\text{ h}^{-1}$ and $\text{V}(\text{HCl})/\text{V}(\text{C}_2\text{H}_2) = 1.2$.

Table 1
Texture parameters of samples.

Sample	$S_{\text{BET}} (\text{m}^2 \cdot \text{g}^{-1})^{[a]}$		$V_{\text{total}} (\text{cm}^3 \cdot \text{g}^{-1})^{[b]}$	
	Fresh	Spent	Fresh	Spent
AC	1374	1347	0.48	0.50
10%[DBU][Cl]/AC	1092	1117	0.39	0.44
20%[DBU][Cl]/AC	486	793	0.29	0.37
30%[DBU][Cl]/AC	228	386	0.24	0.34
40%[DBU][Cl]/AC	92	119	0.16	0.20

[a] BET specific surface area. [b] Total pore volume by BJH desorption.

for the catalytic activity and extends the catalyst's life. For example, Zhu et al. designed a catalyst of B and N heteroatoms codoped on oxide graphene, which showed acetylene conversion of 94.87% [2]. Temperature-programmed desorption (TPD) and DFT calculations indicated that the high catalytic activity was attributed to the enhanced HCl adsorption capacity due to the synergistic effect of B and N atoms. Liu et al. reported a nonmetallic HMT/AC catalyst, which gave ~60% conversion and 99% VCM selectivity [35]. Combining theoretical calculations and characterization analysis, HMT can preferentially adsorb HCl and form a complex (HMT-HCl). In addition, a single component metal-free catalyst was synthesized with an imidazolyl ionic liquid and

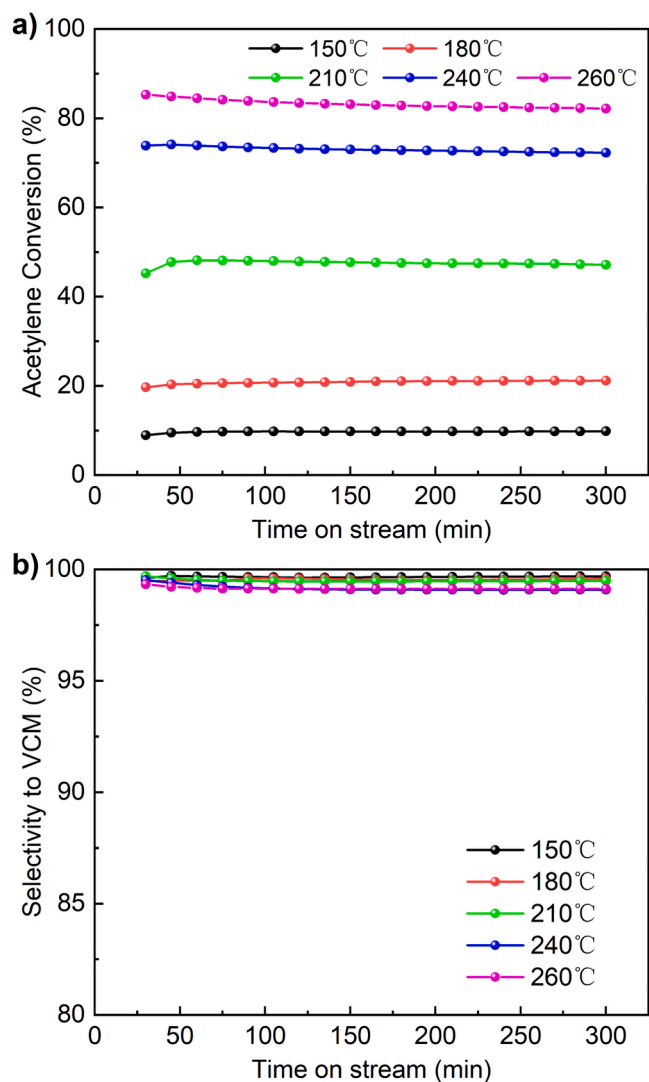


Fig. 2. Acetylene conversion (a) and selectivity to VCM (b) over the 20%[DBU][Cl]/AC catalyst. Reaction conditions: $\text{GHSV}(\text{C}_2\text{H}_2) = 60\text{ h}^{-1}$ and $\text{V}(\text{HCl})/\text{V}(\text{C}_2\text{H}_2) = 1.2$.

the proposed catalytic mechanism indicated that the anion of ionic liquids must be a chloride anion because it participates in acetylene hydrochlorination by the activation of hydrogen chloride molecule [36].

Previous studies reported that DBU could efficiently catalyze the aza-Michael addition reaction [37,38] and nucleophilic addition reaction [39]. It is reasonable that DBU may be active in the hydrochlorination of acetylene. We speculated that functionalized DBU could effectively adsorb and activate hydrogen chloride molecules and catalyze the hydrochlorination of acetylene. Hence, a series of [DBU][Cl]/AC metal-free catalysts were synthesized and studied in depth. The catalytic performance of [DBU][Cl]/AC catalysts was evaluated to specify high catalytic activity and long service life. SEM, BET, XRD, FT-IR and TGA characterization experiments were employed to study the surface morphology, structural properties and thermal stability of the catalysts. Temperature programmed desorption, intermittent flow experiments and theoretical calculations were performed to study the adsorption behavior of reactant and product molecules on [DBU][Cl] and the catalytic mechanism in hydrochlorination of acetylene.

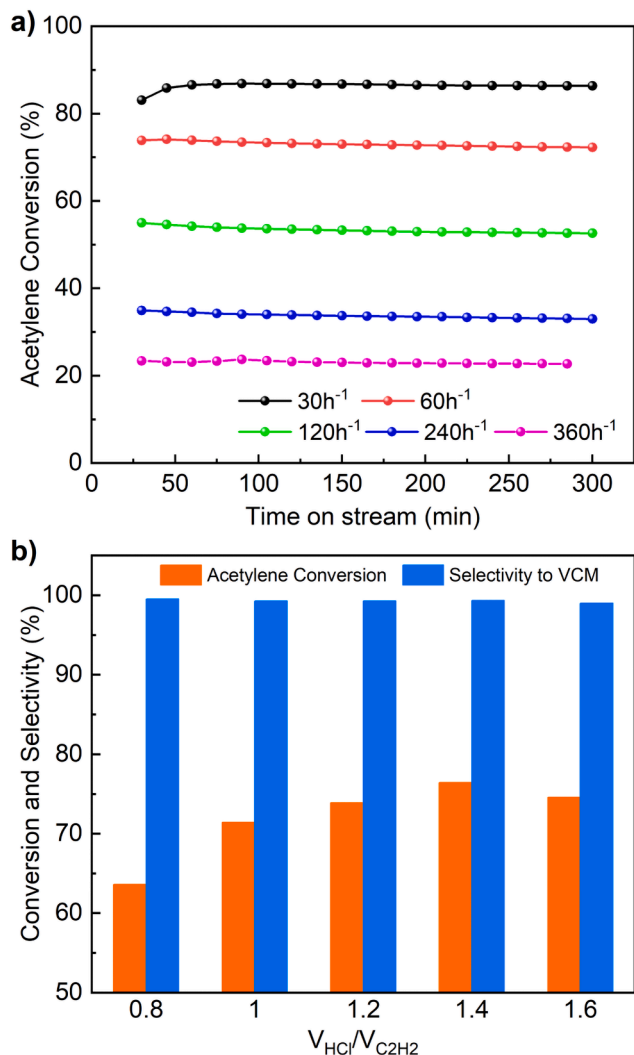


Fig. 3. Acetylene conversion (a) over the 20%[DBU][Cl]/AC catalyst under different GHSV(C_2H_2). Reaction conditions: $T = 240\text{ }^\circ\text{C}$ and $V(\text{HCl})/V(C_2H_2) = 1.2$. Acetylene conversion and selectivity to VCM (b) over the 20%[DBU][Cl]/AC catalyst under different $V(\text{HCl})/V(C_2H_2)$. Reaction conditions: $T = 240\text{ }^\circ\text{C}$ and $\text{GHSV}(C_2H_2) = 60\text{ h}^{-1}$.

2. Experimental

2.1. Materials

Activated carbon (AC, 20–40 mesh) was supplied by Fujian Xinsen Carbon Co., Ltd. Hydrochloric acid (HCl aqueous solution, 36.0–38.0 wt %) was derived from Tianjin Damao Chemical Reagent Factory. Nitric acid (HNO_3 aqueous solution, 65.0–68.0 wt%) was purchased from XiLong Co., Ltd. 1,8-diazabicyclo[5.4.0]undec-7-ene (DBU), 1,5-diazabicyclo[4.3.0]-5-ene (DBN) and 1,5,7-triazabicyclo[4.4.0]dec-5-ene (TBD) were supplied by Shanghai Aladdin Bio-Chem Technology Co., LTD. Acetylene (C_2H_2 , 99.9%) was purchased from Dalian Guangming Special Gases Co., LTD. HCl gas (99.999%) and vinyl chloride gas (10% $C_2H_3Cl + 90\%\text{He}$) were supplied by Dalian Special Gases Co., LTD.

2.2. Catalyst preparation

[DBU][Cl]/AC catalysts were prepared through a wetness impregnation method. Firstly, activated carbon was pretreated by HNO_3 aqueous solution (5 wt%) at $25\text{ }^\circ\text{C}$ to remove impurity metallic elements. Then, AC was washed to $\text{pH} = 7$ with deionized water, dried and

reserved. Next, 1.00 g DBU and 0.65 g hydrochloric acid (5 wt%) were successively dispersed in 6.35 g anhydrous ethanol, and then the mixture was stirred for 10 min to obtain [DBU][Cl] solution. Furthermore, 5.00 g pretreated AC was added into [DBU][Cl] solution under ultrasound and the solid phase was incubated at room temperature for 8–12 h. Finally, the sample was dried at $100\text{ }^\circ\text{C}$ for 12 h to obtain the catalyst, named 20%[DBU][Cl]/AC. In similar way, 10%[DBU][Cl]/AC, 30%[DBU][Cl]/AC and 40%[DBU][Cl]/AC catalysts were prepared, respectively, with the amounts of DBU added 0.50 g, 1.50 g and 2.00 g. The preparation of 20%[DBN][Cl]/AC and 20%[TBD][Cl]/AC catalysts used the same method, except that DBU was substituted for DBN and TBD.

2.3. Catalyst characterizations

The structural properties of samples were studied by N_2 adsorption/desorption isotherms at 77K using Micromeritics GeminiVII. Scanning Electron Microscope (SEM) was conducted on a Hitachi SU8020 instrument to observe morphologies and elemental mappings of the catalysts. The XRD patterns of samples were recorded on an X-ray diffractometer (PANalytical X'Pert PRO) with the Cu-K α radiation ($\lambda = 1.54059\text{ \AA}$) at 40 kV and 40 mA. Fourier transform infrared spectra (FT-IR) of samples were measured from 500 cm^{-1} to 2000 cm^{-1} using Thermofisher scientific Nicolet iS50. The adsorption and desorption properties of reactants and products on catalysts were investigated by Temperature-programmed desorption (TPD) experiments using Micromeritics Chemisorption Analyzer Auto Chem 2920. The thermogravimetry analysis (TGA) was employed to probe the thermal stability and carbon deposition of catalysts on TA Instrument SDT-650 analyzer. Thermal analysis was performed at a heating rate of $10\text{ }^\circ\text{C}/\text{min}$ from $25\text{ }^\circ\text{C}$ to $800\text{ }^\circ\text{C}$ under an air flow of 100 ml/min.

2.4. Catalysts test

The acetylene hydrochlorination performance of samples were evaluated in a fixed-bed reactor (i.d. 10 mm). C_2H_2 gas (0.1 MPa) and HCl gas (0.1 MPa) were fed through mass flow meters into a special steel reactor with 5 ml samples. The catalyst was dried for 2 h at $200\text{ }^\circ\text{C}$ with high purity nitrogen to remove air and moisture and then activated by hydrogen chloride at reaction temperature for 30 min before the reaction started. The temperature controller was employed to conduct the temperature of the catalyst bed. Gas-phase products were analyzed by Agilent 7890B GC with flame ionization detector (FID). The final effluent passed absorption tower containing activated carbon and 13X zeolite to absorb unreacted acetylene, hydrogen chloride and other environmentally harmful products.

Intermittent flow experiment: Fed HCl into the reactor at 12 ml/min for 2 h and then purge residual HCl with N_2 for 2 h. Then, acetylene gas was fed to the reactor at a rate of 5 ml/min and acetylene conversion was recorded.

2.5. Computational details

DFT calculations were carried out in Gaussian 09 computer software package [40]. All molecular geometries involved in the reaction path were optimized without any restrictions. Geometry optimizations, frequency calculations and single-point energy calculations were carried out using the Becke-3-Lee-Yang-Parr (B3LYP) [41–43] method. In geometric optimization and single-point energy calculations, 6-311G (d, p) basis set was applied to all atoms. The intrinsic reaction coordinate (IRC) [44,45] of transition states were calculated at the same level. Atomic charges were endowed with the Mulliken type. Transition states (one imaginary frequency) and minima (no imaginary frequencies) were determined through all stagnation points. The sum of the electronic and zero-point energies was defined as energy values (E) in this study. The adsorption energies (E_{ads}) were calculated as shown in Eq. (1).

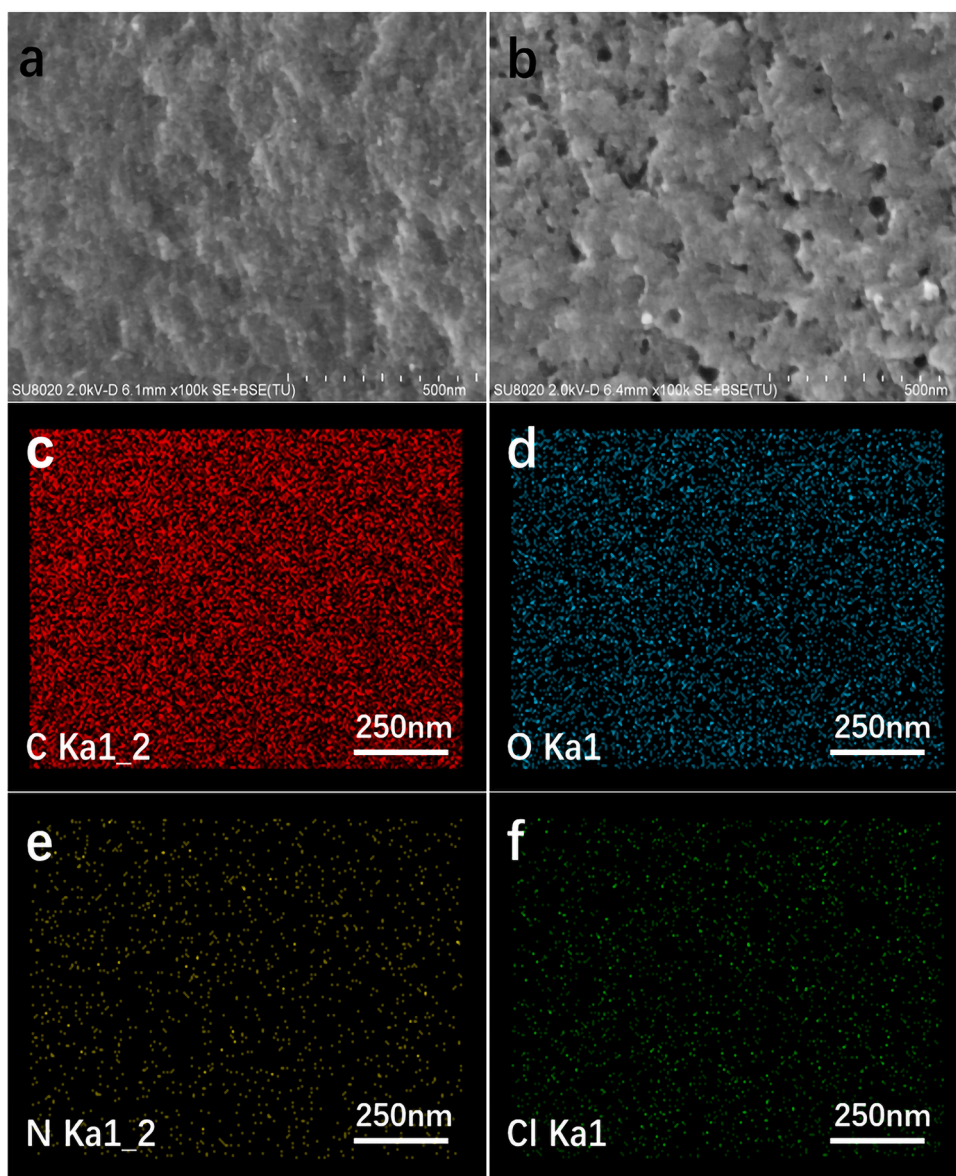


Fig. 4. SEM images of AC (a) and 20%[DBU][Cl]/AC (b) and elemental mapping images of C (c), O (d), N (e) and Cl (f) of 20%[DBU][Cl]/AC.

$$E_{ads} = E_{adsorption} - E_{molecule} - E_{[DBU][Cl]} \quad (1)$$

where $E_{molecule}$ refers the energy of free HCl, C_2H_2 or VCM, respectively.

3. Results and discussion

3.1. Catalytic performance of [DBU][Cl]/AC catalysts

The catalytic performance of [DBU][Cl]/AC catalysts was tested in a fixed-bed reactor. Fig. 1a shows the acetylene conversion of samples with different [DBU][Cl] loadings. The initial acetylene conversion of AC is only 30.4% and it is reduced to 19.4% after 300 min of evaluation. The rapid deactivation rate of AC may be due to coke deposition [46]. In contrast, the initial acetylene conversion is significantly increased after the introduction of [DBU][Cl] and it reaches 85.5% for the 40% [DBU][Cl]/AC catalyst. The low specific surface area (Table 1) of 40%[DBU][Cl]/AC should be attributed to agglomeration and pore occupancy of active components. Therefore, the higher acetylene conversion of 40% [DBU][Cl]/AC suggests that it exposes more active sites. Moreover, the acetylene conversion of all [DBU][Cl]/AC catalysts slightly decreases after the same evaluation time. This implies that the introduction of

[DBU][Cl] can not merely strengthen catalytic activity, but also improve the stability of [DBU][Cl]/AC samples. Fig. 1b shows that the selectivity to VCM is above 99% for all [DBU][Cl]/AC catalysts. To further investigate the effect of bed temperature on catalyst performance, 20%[DBU][Cl]/AC was tested under different bed temperatures. In Fig. 2, in the range of 150–260 °C, the acetylene conversion of 20%[DBU][Cl]/AC has a significant positive correlation with bed temperature, and the selectivity to VCM is hardly affected by bed temperature. The acetylene conversion is the highest (85.3%) when the bed temperature is 260 °C. Taking into account the thermal decomposition of [DBU][Cl] and energy consumption at high temperature, the optimal temperature was determined to be 240 °C. Fig. 3a shows the acetylene hydrochlorination of the 20%[DBU][Cl]/AC catalyst at different GHSV(C_2H_2). The acetylene conversion reaches 86.8%, and the selectivity is always above 99.5% under the condition close to the industrial GHSV(C_2H_2) of 30 h^{-1} . Next, the 20%[DBU][Cl]/AC catalyst was evaluated under different feed gas ratios. Fig. 3b demonstrates that the acetylene conversion increases and then decreases with $V(HCl)/V(C_2H_2)$ enhancement from 0.8 to 1.4. The $V(HCl)/V(C_2H_2)$ ratio of 1.2 is determined to be the best value from the perspective of the utilization rate of HCl and environmental friendliness. The chemical structures of [DBN][Cl] and [TBD][Cl] are

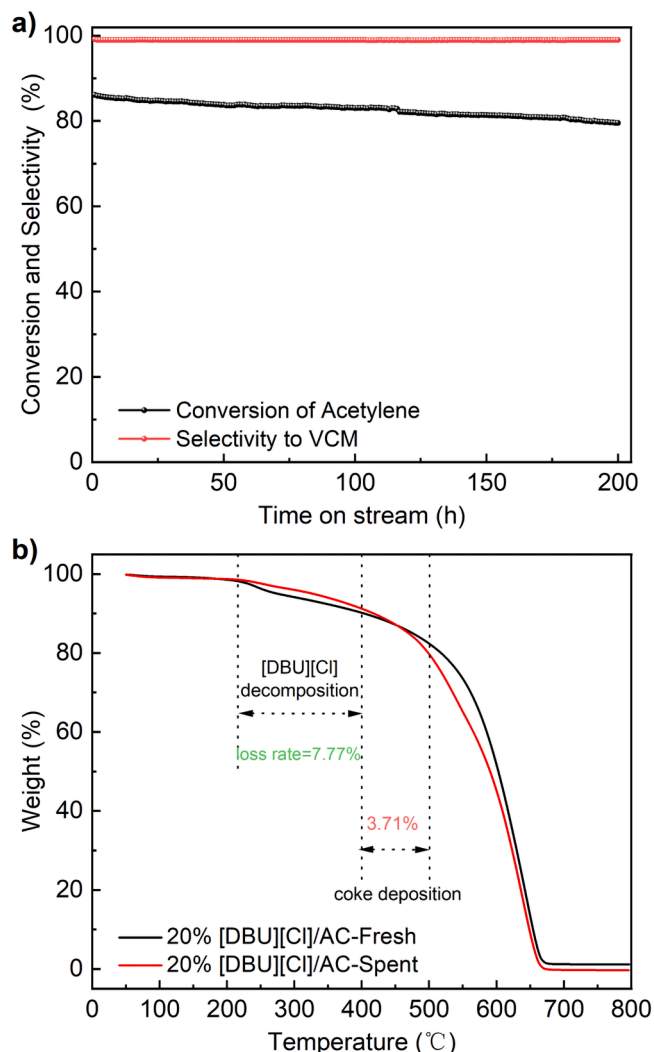


Fig. 5. Acetylene conversion and selectivity to VCM (a) over the 20%[DBU][Cl]/AC catalyst. $T = 240\text{ }^{\circ}\text{C}$, $\text{GHSV}(\text{C}_2\text{H}_2) = 30\text{ h}^{-1}$ and $V(\text{HCl})/V(\text{C}_2\text{H}_2) = 1.2$. TGA profiles(b) of the fresh and spent 20%[DBU][Cl]/AC catalysts in an air atmosphere.

close to that of [DBU][Cl] (Fig. S2). The catalytic performance of 20% [DBN][Cl]/AC and 20%[TBD][Cl]/AC was evaluated at $T = 240\text{ }^{\circ}\text{C}$, $\text{GHSV}(\text{C}_2\text{H}_2) = 60\text{ h}^{-1}$ and $V(\text{HCl})/V(\text{C}_2\text{H}_2) = 1.2$. Acetylene conversion is 78.1% and 66.0% on 20%[DBN][Cl]/AC and 20%[TBD][Cl]/AC, respectively, and the selectivity to VCM is above 99% (Fig. S1).

3.2. Characterization of the [DBU][Cl]/AC catalysts

Fig. 4a, b show scanning electron microscopy (SEM) images of AC and 20%[DBU][Cl]/AC, in which a fluffy porous structure is displayed. Fig. 4c–f exhibit a uniform distribution of carbon, oxygen, nitrogen and chlorine elements on the 20%[DBU][Cl]/AC surface, indicating the uniform dispersion of [DBU][Cl] on AC support. The surface element composition of AC and the 20%[DBU][Cl]/AC catalyst was confirmed by SEM-EDX, as listed in Table S1. The structural properties of samples were studied by N_2 adsorption/desorption isotherms at 77 K. Fig. S3 shows that all the samples have a type IV adsorption isotherm because of the adsorption hysteresis loop. Table 1 lists the specific surface area and total pore volume of fresh and spent samples. For fresh samples, the specific surface area decreases from $1374\text{ m}^2/\text{g}$ to $92\text{ m}^2/\text{g}$ and pore volume decreases from $0.48\text{ m}^3/\text{g}$ to $0.16\text{ m}^3/\text{g}$, respectively, when the loading of [DBU][Cl] increases from 0 to 40%. The decrease is due to

partial micropores of AC being occupied by [DBU][Cl]. Although the specific surface area of 40%[DBU][Cl]/AC is reduced to $92\text{ m}^2/\text{g}$, its catalytic activity is the highest, which also confirms that [DBU][Cl] is indeed the active site of acetylene conversion. Compared to the fresh sample, the reduced specific surface area of spent AC is owing to coke deposition during acetylene hydrochlorination [47]. In contrast, for the spent [DBU][Cl] catalysts, the specific surface areas surprisingly increase after evaluation, compared to the fresh individual counterparts. The increased specific surface area suggests that there is a partial loss of [DBU][Cl] component during the reaction process. Fig. S4 displays the XRD patterns for fresh AC and 20%[DBU][Cl]/AC samples. The peaks situated at 23.3° and 43.6° are characteristic of the (0 0 2) and (1 0 1) planes of graphitic carbon [48]. Fig. S5 displays the FT-IR spectra of AC, 20%[DBU][Cl]/AC and [DBU][Cl]. The absorption peaks at 1645 cm^{-1} and 1321 cm^{-1} are assigned to the stretching vibration of the C=N bond and the out-of-plane bending vibration of the C-H bond in the spectrum of [DBU][Cl] [49]. Two identical peaks are also found in the spectrum of 20%[DBU][Cl]/AC, indicating that [DBU][Cl] is only anchored to AC by adsorption without other chemical changes or decomposition.

3.3. The lifetime test and thermogravimetric analysis of 20%[DBU][Cl]/AC

The service life of the catalyst is a significant parameter in the industrial process of acetylene hydrochlorination. The life test of the 20% [DBU][Cl]/AC catalyst was performed under the conditions of $T = 240\text{ }^{\circ}\text{C}$, $\text{GHSV}(\text{C}_2\text{H}_2)$ of 30 h^{-1} and $V(\text{HCl})/V(\text{C}_2\text{H}_2)$ of 1.2. As can be seen from Fig. 5a, the initial acetylene conversion reaches 86.1%, and the VCM selectivity is above 99.2%. The acetylene conversion merely decreases to 79.5%, and the deactivation rate is only 0.033 %/h within 200 h. The catalytic performance data of 20%[DBU][Cl]/AC and reported nonmetallic catalysts are listed in Table S2. This implies that the 20%[DBU][Cl]/AC catalyst could be a promising mercury-free catalyst for acetylene hydrochlorination. TGA was further carried out to explore the thermal stability and deactivation cause of the 20%[DBU][Cl]/AC catalyst. Fig. S6 shows that the thermal decomposition of [DBU][Cl] occurs in 220–400 $^{\circ}\text{C}$ in an air atmosphere. TGA profiles of the fresh and spent 20%[DBU][Cl]/AC tested for 200 h are displayed in Fig. 5b. The weight loss peak between 220 $^{\circ}\text{C}$ and 400 $^{\circ}\text{C}$ is due to the thermal decomposition of [DBU][Cl] on the basis of TGA profile of [DBU][Cl]. Compared with the fresh 20%[DBU][Cl]/AC sample, the weight loss of the spent 20%[DBU][Cl]/AC catalyst is significantly reduced at 220–400 $^{\circ}\text{C}$, which indicates that part of [DBU][Cl] is lost and the loss rate is 7.77% during the reaction progresses. The mass loss above 500 $^{\circ}\text{C}$ belongs to combustion decomposition of AC support in air atmosphere [3,50]. The weight loss difference between the spent and fresh 20% [DBU][Cl]/AC catalysts at 400–500 $^{\circ}\text{C}$ could reflect coke deposition [51]. The amount of coke deposition was 3.71% during the 200 h evaluation. On the basis of above results, we summarized that the deactivation of the 20%[DBU][Cl]/AC catalyst in the 200 h evaluation was attributed to the loss of a small part of [DBU][Cl] and carbon deposition.

3.4. The adsorption properties of reactants/products on 20%[DBU][Cl]/AC

TPD characterizations were performed to investigate the adsorption behaviors of reactant and product molecules on the 20%[DBU][Cl]/AC catalyst. In Fig. 6a, the TPD-He profile of 20%[DBU][Cl]/AC shows that the desorption peak located at 410 $^{\circ}\text{C}$ ascribes the thermal decomposition of [DBU][Cl]. Fig. 6b–d display TPD- C_2H_2 , TPD-HCl, and TPD-VCM profiles of the AC and 20%[DBU][Cl]/AC samples. Generally, the desorption peak temperature represents the adsorption strength between the adsorbate and adsorbent, and the desorption peak area is related to the adsorption amount in the TPD profiles [52,53]. Compared with the AC support, the C_2H_2 desorption peak of the 20%[DBU][Cl]/AC

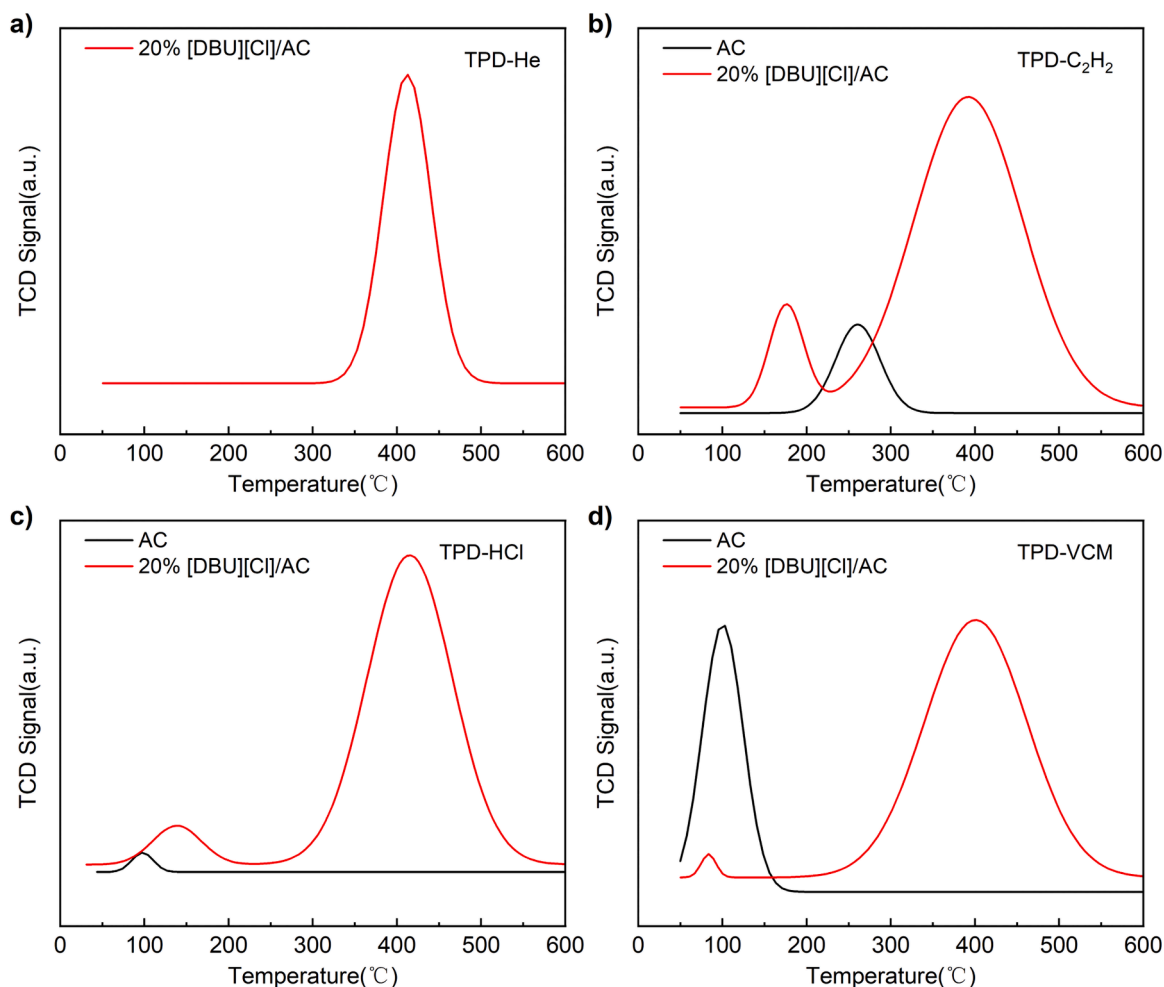


Fig. 6. TPD profiles of the fresh 20%[DBU][Cl]/AC and AC catalysts. (a) TPD-He, (b) TPD-C₂H₂, (c) TPD-HCl and (d) TPD-VCM.

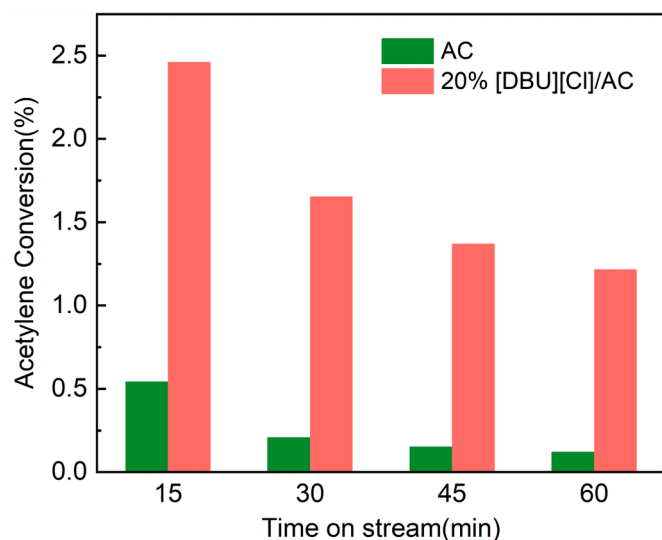


Fig. 7. Intermittent flow experiments over 20%[DBU][Cl]/AC and AC catalysts. (HCl: 12 ml/min, 2 h → N₂: 20 ml/min, 2 h → C₂H₂: 5 ml/min, recording).

catalyst moves to a lower temperature. This indicates that [DBU][Cl] can reduce the adsorption strength of C₂H₂ and positively affect the deactivation of the 20%[DBU][Cl]/AC catalyst. It was demonstrated in a

Table 2

The adsorption energy of C₂H₂, HCl and VCM on [DBU][Cl], [DBN][Cl] and [TBD][Cl] (kcal/mol).

	C ₂ H ₂	HCl	VCM
[DBU][Cl]	-4.89	-11.07	-3.68
[DBN][Cl]	-4.50	-11.81	-3.90
[TBD][Cl]	-4.25	-10.48	-3.58

Table 3

Charge variations in the atoms of C₂H₂, HCl and C₂H₃Cl adsorbed on [DBU][Cl].

Molecule	Atoms	Before adsorption (e)	After adsorption (e)	Δ (e)	Δ(e) (molecule)
C ₂ H ₂	H1	0.121	0.171	0.050	-0.017
	C1	-0.121	-0.086	0.035	
	H2	0.121	0.110	-0.011	
	C2	-0.121	-0.212	-0.091	
HCl	H	0.176	0.215	0.039	-0.171
	Cl	-0.176	-0.386	-0.210	
C ₂ H ₃ Cl	H1	0.128	0.122	-0.006	-0.022
	H2	0.135	0.200	0.065	
	C1	-0.158	-0.157	0.001	
	C2	-0.21	-0.221	-0.011	
	H3	0.169	0.164	-0.005	
	Cl	-0.063	-0.129	-0.066	

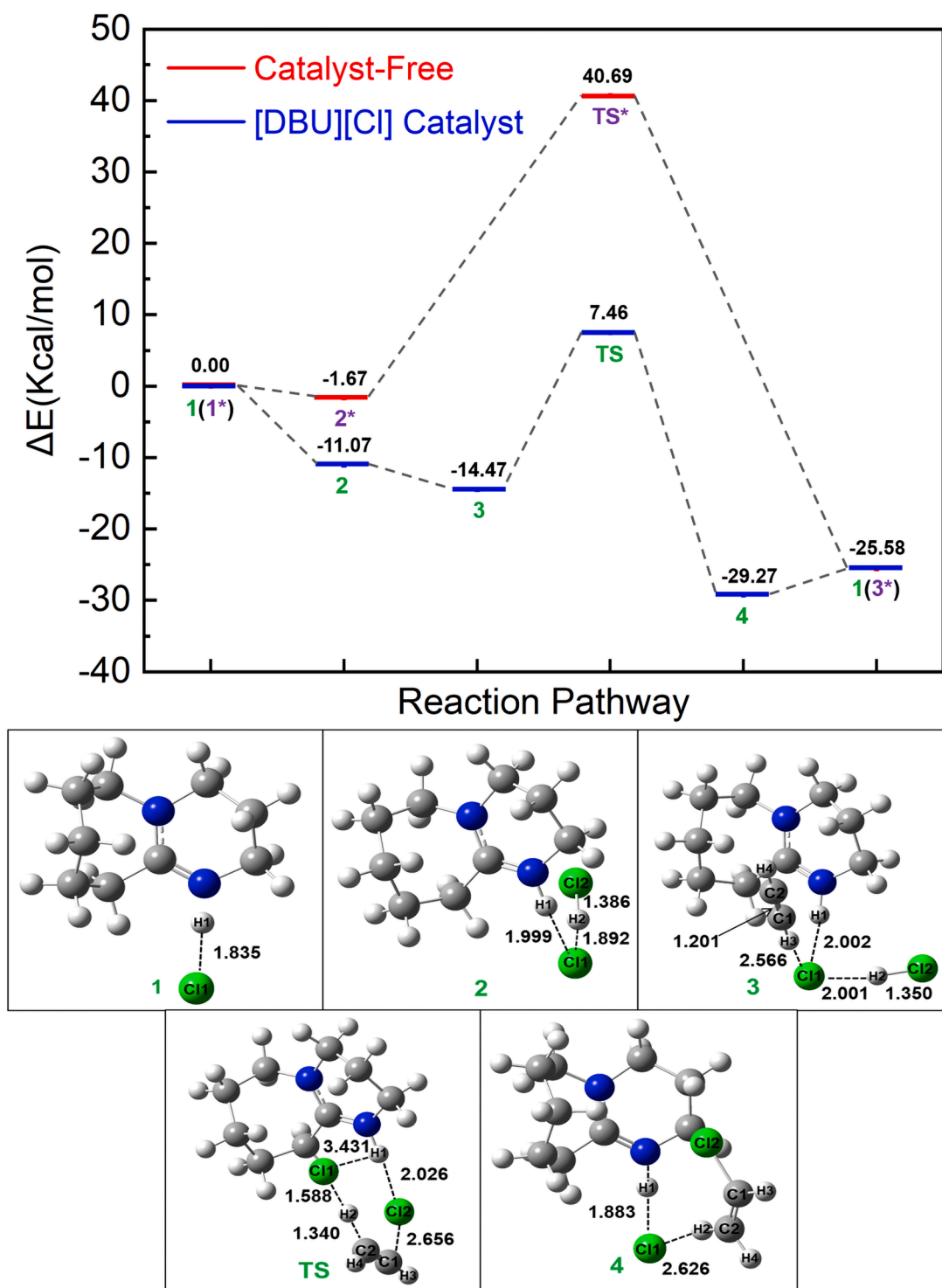
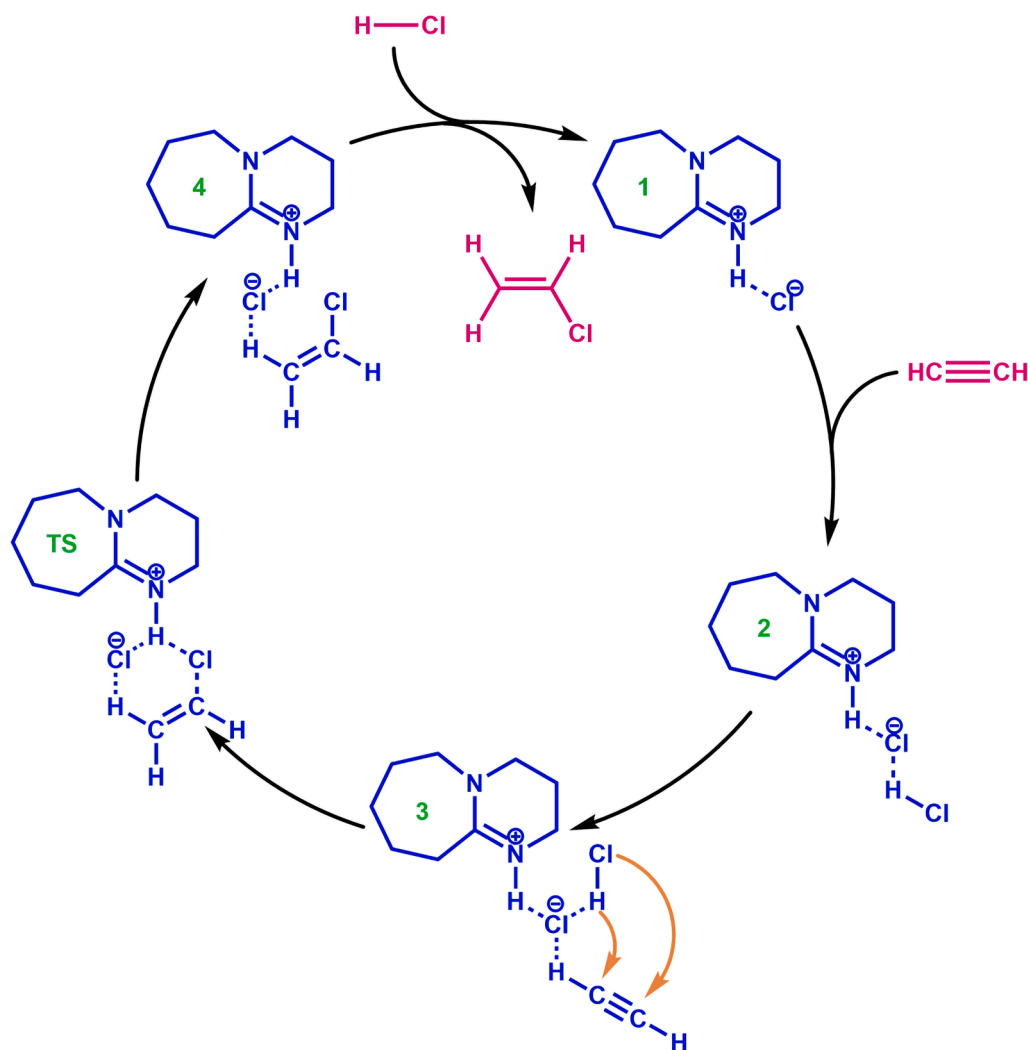


Fig. 8. Reaction energy diagram and the geometric structures of the substances involved in the reaction pathways. Carbon, hydrogen, nitrogen and chlorine atoms are depicted in gray, white, blue and green, respectively.

number of studies that a reduction in C_2H_2 adsorption strength could inhibit the occurrence of side reactions and the formation of carbon deposition [21,47]. For the HCl reactant, the desorption peak area and position on 20%[DBU][Cl] are larger than those on AC, implying a larger HCl adsorption capacity and strength on the 20%[DBU][Cl]/AC catalyst. Much work has reported that a high adsorption capacity and adsorption strength promote the adsorption of HCl molecules, which has a positive effect on the catalytic activity of 20%[DBU][Cl]/AC [25,48,

54]. For the VCM product, the VCM desorption peak area on 20%[DBU][Cl]/AC is smaller than that on AC. This means that VCM can desorb quickly from the catalyst surface, which greatly improves the turnover frequency of the reactant molecules and resists the formation of coke deposition [47,48]. Comparing the TPD results of 20%[DBU][Cl]/AC with those of AC, it can be recognized that the increased HCl and decreased VCM adsorption capacity and the weak C_2H_2 adsorption strength of 20%[DBU][Cl]/AC can be attributed to the addition of



Scheme 1. The catalytic mechanism of acetylene hydrochlorination over [DBU][Cl] site.

[DBU][Cl]. From the above results, it can be summarized that [DBU][Cl] can not only enhance the catalytic activity but also improve stability [3, 55]. To further verify that the HCl adsorption capacity on 20%[DBU][Cl] is higher than that on AC, we conducted intermittent flow experiments. Fig. 7 shows that the acetylene conversion of 20%[DBU][Cl]/AC is always greater than that of AC at the same moment, which reveals that the 20%[DBU][Cl]/AC catalyst has a larger HCl storage capacity than the AC support. The weaker adsorption of vinyl chloride may also have a positive effect on the improvement of VCM amount produced by 20% [DBU][Cl]/AC. This result is consistent with the result from TPD-HCl.

3.5. The catalytic mechanism of acetylene hydrochlorination over [DBU][Cl] site

To further understand the reaction mechanism of acetylene hydrochlorination catalyzed by [DBU][Cl], we executed a series of DFT calculations. Table 2 displays that the adsorption energies (E_{ads}) of C_2H_2 , HCl and VCM on [DBU][Cl] are -4.89, -11.07 and -3.68 kcal/mol, respectively. The results prove that [DBU][Cl] prefers to adsorb HCl rather than C_2H_2 by the more negative adsorption energy. The adsorption energies of reactants/products on [DBN][Cl] and [TBD][Cl] are essentially comparable to their adsorption energies on [DBU][Cl]. This preferential adsorption of HCl not merely enhances the catalytic activity, but also inhibits the deactivation of the catalyst [46,47]. Previous reports identified that B, N-G had higher HCl adsorption energy than

N-G, implying that the catalyst improved acetylene hydrochlorination [2]. Meanwhile, the lower adsorption energy makes for the rapid desorption of VCM from the internal pore of catalyst. As listed in Table 3, the electrons transferred are 0.017 e, 0.171 e and 0.022 e from [DBU][Cl] to C_2H_2 , HCl and VCM by Mulliken charge analysis. It is clearly illustrated that [DBU][Cl] tends to transfer more electrons to HCl than C_2H_2 and VCM. This result is consistent with the adsorption energy (E_{ad}), indicating that [DBU][Cl] preferentially activates HCl molecules rather than C_2H_2 [35]. Fig. 8 shows the probable reaction pathway over [DBU][Cl] and involved ground-state structures in the reaction pathway, including the [DBU][Cl] initial configuration (1), HCl adsorption on the [DBU][Cl] configuration (2), HCl and C_2H_2 co-adsorption on the [DBU][Cl] configuration (3), transition state configuration (TS), and VCM adsorption on the [DBU][Cl] configuration (4). In the HCl adsorption on the [DBU][Cl] configuration, the H2 atom from the HCl molecule gradually moves to the Cl1 anion of [DBU][Cl] to form a H2-Cl1 bond because of a hydrogen bond interaction, with a bond length of 1.892 Å. Meanwhile, the bond lengths of H1-Cl1 and H2-Cl2 stretch to 1.999 Å and 1.386 Å, respectively. The E_{ad} of HCl adsorption on [DBU][Cl] is -11.07 kcal/mol. In the HCl and C_2H_2 coadsorption on the [DBU][Cl] configuration, the H3 atom in the C_2H_2 molecule draws near the Cl1 anion, the distance between H3 and Cl1 is 2.566 Å, and the bond length of H2-Cl1 slightly stretches to 2.001 Å. The E_{ad} of C_2H_2 adsorption on the [DBU][Cl]-HCl complex is -3.40 kcal/mol. In the transition state configuration, H2 and Cl2 atoms attack C2 and C1 atoms,

respectively, with bond lengths of H2-C2 and Cl2-C1 of 1.340 Å and 2.656 Å, respectively. The relative energy of the transition state is 7.46 kcal/mol. In the VCM adsorption on the [DBU][Cl] configuration, the bond lengths of H2-C2 and Cl2-C1 are further shortened to 1.087 Å and 1.773 Å which are equal to the bond lengths of H-C (1.083 Å) and Cl-C (1.754 Å) in the free VCM molecule. Finally, the desorption of VCM from the [DBU][Cl] catalyst is quite facile with only 3.69 kcal/mol energy, inhibiting the progress of side reactions and reducing the formation of coke deposition. To verify the rationality of TS, the intrinsic reaction coordinate (IRC) was executed and the outcomes are exhibited in Fig. S8. The TS has only one imaginary frequency (-612.32 cm^{-1}), corresponding to the stretching vibration of the H2 between C2 and Cl1 and the bending vibration of the H4 and H3. The initial state calculated by IRC is the HCl and C₂H₂ coadsorption on the [DBU][Cl] configuration, and the final state calculated by IRC is the VCM adsorption on the [DBU][Cl] configuration. The above results prove that the transition state structure is reasonable. In the present of [DBU][Cl], the energy barrier is only 21.93 kcal/mol. In addition, Figs. 8 and S7 also show the acetylene hydrochlorination pathway without the catalyst, including the reactant (1*), C₂H₂-HCl adsorption state (2*), transition state (TS*) and product (3*). In defect of the catalyst, the energy barrier is up to 42.36 kcal/mol in acetylene hydrochlorination. Comparing the energy barriers between the [DBU][Cl] catalyst and catalyst-free cases, we conclude that the addition of [DBU][Cl] can obviously reduce the activation energy. In brief, the preferential adsorption and activation of HCl on [DBU][Cl] and the reduction of activation energy will facilitate satisfactory catalytic activity and stability [56]. The catalytic cycle of acetylene hydrochlorination over [DBU][Cl] active site is shown in Scheme 1.

4. Conclusions

[DBU][Cl]/AC catalysts for acetylene hydrochlorination were systematically investigated in this work. It was first found that nitrogen-containing diheterocyclic molecule, [DBU][Cl], exhibited excellent catalytic performances. The acetylene conversion and the selectivity to VCM are 86.8% and 99.5%, respectively, and the deactivation rate is only 0.033 %/h during the 200 h lifetime evaluation over the 20%[DBU][Cl]/AC catalyst under the reaction conditions of T = 240 °C, GHSV (C₂H₂) = 30 h⁻¹ and V(HCl)/V(C₂H₂) = 1.2. To reveal the catalytic mechanism, a variety of characterizations and experiments were executed on the 20%[DBU][Cl]/AC catalyst and AC support, including SEM, BET, XRD, FT-IR, TGA, TPD and intermittent feeding experiments. The analysis of characterization results indicated that the good catalytic activity and stability could be ascribed the larger HCl and smaller VCM adsorption capacity as well as weaker C₂H₂ adsorption strength of the catalyst. Furthermore, DFT calculations demonstrated that [DBU][Cl] could transfer more electrons (-0.171 e) to HCl and had the lowest adsorption energy (-11.07 kcal/mol) compared to C₂H₂ and VCM. As a result, [DBU][Cl] could preferentially adsorb and activate HCl molecules in acetylene hydrochlorination. In addition, the apparent activation energy is only 21.93 kcal/mol over [DBU][Cl] site, theoretically confirming the good activity of the [DBU][Cl]/AC catalyst in acetylene hydrochlorination.

CRedit authorship contribution statement

Xingzong Dong: Conceptualization, Software, Investigation, Writing – original draft. **Guangye Liu:** Investigation, Resources, Supervision. **Zhaoran Chen:** Software, Formal analysis. **Quan Zhang:** Formal analysis. **Yunpeng Xu:** Project administration, Writing – review & editing, Funding acquisition. **Zhongmin Liu:** Project administration, Funding acquisition.

Declaration of Competing Interest

The authors declare that they have no known competing financial interests or personal relationships that could have appeared to influence the work reported in this paper.

Acknowledgments

This work was supported by Key Technologies Research and Development Program [2016YFB0301603] and Liaoning Revitalization Talents Program [XLYC1905017].

Supplementary materials

Supplementary material associated with this article can be found, in the online version, at doi:10.1016/j.mcat.2022.112366.

References

- [1] P. Johnston, N. Carthey, G.J. Hutchings, Discovery, development, and commercialization of gold catalysts for acetylene hydrochlorination, *J. Am. Chem. Soc.* 137 (2015) 14548–14557, <https://doi.org/10.1021/jacs.5b07752>.
- [2] B. Dai, K. Chen, Y. Wang, L. Kang, M. Zhu, Boron and nitrogen doping in graphene for the catalysis of acetylene hydrochlorination, *ACS Catal.* 5 (2015) 2541–2547, <https://doi.org/10.1021/acscatal.5b00199>.
- [3] S. Shang, W. Zhao, Y. Wang, X. Li, J. Zhang, Y. Han, W. Li, Highly efficient Ru@IL/AC to substitute mercuric catalyst for acetylene hydrochlorination, *ACS Catal.* 7 (2017) 3510–3520, <https://doi.org/10.1021/acscatal.7b00057>.
- [4] G.J. Hutchings, Vapor-phase hydrochlorination of acetylene - correlation of catalytic activity of supported metal chloride catalysts, *J. Catal.* 96 (1985) 292–295, [https://doi.org/10.1016/0021-9517\(85\)90383-5](https://doi.org/10.1016/0021-9517(85)90383-5).
- [5] X. Li, M. Zhu, B. Dai, AuCl₃ on polypyrrole-modified carbon nanotubes as acetylene hydrochlorination catalysts, *Appl. Catal. B* 142–143 (2013) 234–240, <https://doi.org/10.1016/j.apcatb.2013.05.031>.
- [6] S.A. Mitchenko, E.V. Khomutov, A.A. Shubin, Y.M. Shul'ga, Catalytic hydrochlorination of acetylene by gaseous HCl on the surface of mechanically pre-activated K₂PtCl₆ salt, *J. Mol. Catal. A Chem.* 212 (2004) 345–352, <https://doi.org/10.1016/j.molcata.2003.11.021>.
- [7] S.A. Mitchenko, T.V. Krasnyakova, R.S. Mitchenko, A.N. Korduban, Acetylene catalytic hydrochlorination over powder catalyst prepared by pre-milling of K₂PtCl₆ salt, *J. Mol. Catal. A Chem.* 275 (2007) 101–108, <https://doi.org/10.1016/j.molcata.2007.05.036>.
- [8] S.A. Mitchenko, E.V. Khomutov, A.A. Shubin, I.P. Beletskaya, Estimates of the catalytic efficiency of a heterogeneous catalyst for acetylene hydrochlorination on the surface of mechanically activated K₂PtCl₆ salt, *Kinet. Catal.* 45 (2004) 391–393, <https://doi.org/10.1023/B:KICA.0000032174.71487.ee>.
- [9] Q.L. Song, S.J. Wang, B.X. Shen, J.G. Zhao, Palladium-based catalysts for the hydrochlorination of acetylene: reasons for deactivation and its regeneration, *Pet. Sci. Technol.* 28 (2010) 1825–1833, <https://doi.org/10.1080/10916460903160842>.
- [10] T.V. Krasnyakova, I.V. Zhikharev, R.S. Mitchenko, V.I. Burkhovetski, A. M. Korduban, T.V. Kryshchuk, S.A. Mitchenko, Acetylene catalytic hydrochlorination over mechanically pre-activated K₂PdCl₄ salt: a study of the reaction mechanism, *J. Catal.* 288 (2012) 33–43, <https://doi.org/10.1016/j.jcat.2011.12.020>.
- [11] Y. Pu, J. Zhang, L. Yu, Y. Jin, W. Li, Active ruthenium species in acetylene hydrochlorination, *Appl. Catal. A* 488 (2014) 28–36, <https://doi.org/10.1016/j.apcata.2014.09.037>.
- [12] Y. Han, M. Sun, W. Li, J. Zhang, Influence of chlorine coordination number on the catalytic mechanism of ruthenium chloride catalysts in the acetylene hydrochlorination reaction: a DFT study, *PCCP* 17 (2015) 7720–7730, <https://doi.org/10.1039/c5cp00231a>.
- [13] X.L. Wang, G.J. Lan, H.Z. Liu, Y.H. Zhu, Y. Li, Effect of acidity and ruthenium species on catalytic performance of ruthenium catalysts for acetylene hydrochlorination, *Catal. Sci. Technol.* 8 (2018) 6143–6149, <https://doi.org/10.1039/c8cy01677a>.
- [14] K. Zhou, J. Si, J. Jia, J. Huang, J. Zhou, G. Luo, F. Wei, Reactivity enhancement of N-CNTs in green catalysis of C₂H₂ hydrochlorination by a Cu catalyst, *RSC Adv.* 4 (2014) 7766–7769, <https://doi.org/10.1039/c3ra46099a>.
- [15] Y. Hu, Y. Wang, Y. Wang, W. Li, J. Zhang, Y. Han, High performance of supported Cu-based catalysts modulated via phosphamido coordination in acetylene hydrochlorination, *Appl. Catal. A* 591 (2020), 117408, <https://doi.org/10.1016/j.apcata.2020.117408>.
- [16] K. Zhou, J.C. Jia, X.G. Li, X.D. Pang, C.H. Li, J. Zhou, G.H. Luo, F. Wei, Continuous vinyl chloride monomer production by acetylene hydrochlorination on Hg-free bismuth catalyst: from lab-scale catalyst characterization, catalytic evaluation to a pilot-scale trial by circulating regeneration in coupled fluidized beds, *Fuel Process. Technol.* 108 (2013) 12–18, <https://doi.org/10.1016/j.fuproc.2012.03.018>.

- [17] D. Hu, F. Wang, J. Wang, Bi/AC modified with phosphoric acid as catalyst in the hydrochlorination of acetylene, *RSC Adv.* 7 (2017) 7567–7575, <https://doi.org/10.1039/c6ra26845e>.
- [18] K. Zhou, J. Jia, C. Li, H. Xu, J. Zhou, G. Luo, F. Wei, A low content Au-based catalyst for hydrochlorination of C_2H_2 and its industrial scale-up for future PVC processes, *Green Chem.* 17 (2015) 356–364, <https://doi.org/10.1039/c4gc00795f>.
- [19] J. Li, H. Zhang, L. Li, M. Cai, Y. Li, D. Xie, J. Zhang, Synergistically catalytic hydrochlorination of acetylene over the highly dispersed ru active species embedded in p-containing ionic liquids, *ACS Sustain. Chem. Eng.* 8 (2020) 10173–10184, <https://doi.org/10.1021/acssuschemeng.0c02329>.
- [20] X. Wang, M. Zhu, B. Dai, Effect of phosphorus ligand on cu-based catalysts for acetylene hydrochlorination, *ACS Sustain. Chem. Eng.* 7 (2019) 6170–6177, <https://doi.org/10.1021/acssuschemeng.8b06379>.
- [21] Y. Liu, H. Zhang, X. Li, L. Wang, Y. Dong, W. Li, J. Zhang, Solvent-assisted synthesis of N-doped activated carbon-based catalysts for acetylene hydrochlorination, *Appl. Catal. A* 611 (2021), 117902, <https://doi.org/10.1016/j.apcata.2020.117902>.
- [22] J. Wang, F. Zhao, C. Zhang, L. Kang, M. Zhu, A novel S, N dual doped carbon catalyst for acetylene hydrochlorination, *Appl. Catal. A* 549 (2018) 68–75, <https://doi.org/10.1016/j.apcata.2017.09.025>.
- [23] S.K. Kaiser, K.S. Song, S. Mitchell, A. Coskun, J. Pérez-Ramírez, Nitrogen-doped carbons with hierarchical porosity via chemical blowing towards long-lived metal-free catalysts for acetylene hydrochlorination, *ChemCatChem* 12 (2020) 1922–1925, <https://doi.org/10.1002/cctc.201902331>.
- [24] X. Li, X. Pan, L. Yu, P. Ren, X. Wu, L. Sun, F. Jiao, X. Bao, Silicon carbide-derived carbon nanocomposite as a substitute for mercury in the catalytic hydrochlorination of acetylene, *Nat. Commun.* 5 (2014) 3688, <https://doi.org/10.1038/ncomms4688>.
- [25] S.L. Chao, F. Zou, F.F. Wan, X.B. Dong, Y.L. Wang, Y.X. Wang, Q.X. Guan, G. C. Wang, W. Li, Nitrogen-doped Carbon Derived from ZIF-8 as a High-performance metal-free catalyst for acetylene hydrochlorination, *Sci. Rep.* 7 (2017) 1–7, <https://doi.org/10.1038/srep39789>.
- [26] W. Liu, M. Zhu, B. Dai, Nitrogen doped nanoflower porous carbon as a nonmetal catalyst for acetylene hydrochlorination, *New J. Chem.* 42 (2018) 20131–20136, <https://doi.org/10.1039/c8nj04410d>.
- [27] F. Zhao, Y. Wang, M.Y. Zhu, L.H. Kang, C-doped boron nitride fullerene as a novel catalyst for acetylene hydrochlorination: a DFT study, *RSC Adv.* 5 (2015) 56348–56355, <https://doi.org/10.1039/c5ra08266h>.
- [28] P. Li, H. Li, X. Pan, K. Tie, T. Cui, M. Ding, X. Bao, Catalytically active boron nitride in acetylene hydrochlorination, *ACS Catal.* 7 (2017) 8572–8577, <https://doi.org/10.1021/acscatal.7b01877>.
- [29] G. Lan, Y. Qiu, J. Fan, X. Wang, H. Tang, W. Han, H. Liu, H. Liu, S. Song, Y. Li, Defective graphene@diamond hybrid nanocarbon material as an effective and stable metal-free catalyst for acetylene hydrochlorination, *Chem. Commun.* 55 (2019) 1430–1433, <https://doi.org/10.1039/c8cc09361j>. Cambridge.
- [30] F. Zhao, L. Kang, The neglected significant role for graphene-based acetylene hydrochlorination catalysts - intrinsic graphene defects, *ChemistrySelect* 2 (2017) 6016–6022, <https://doi.org/10.1002/slct.201700951>.
- [31] Y. Qiu, D. Fan, G. Lan, S. Wei, X. Hu, Y. Li, Generalized reactivity descriptor of defective carbon catalysts for acetylene hydrochlorination: the ratio of sp^2 : sp^3 hybridization, *Chem. Commun.* 56 (2020) 14877–14880, <https://doi.org/10.1039/D0CC06177H>.
- [32] S. Ali, M.B.A. Khan, S.A. Khan, The catalytic performance of metal-free defected carbon catalyst towards acetylene hydrochlorination revealed from first-principles calculation, *Int. J. Quantum Chem.* 120 (2020) e26418, <https://doi.org/10.1002/qua.26418>.
- [33] X. Qiao, Z. Zhou, X. Liu, C. Zhao, Q. Guan, W. Li, Constructing a fragmentary $g-C_3N_4$ framework with rich nitrogen defects as a highly efficient metal-free catalyst for acetylene hydrochlorination, *Catal. Sci. Technol.* 9 (2019) 3753–3762, <https://doi.org/10.1039/C9CY00927B>.
- [34] J. Zhao, B. Wang, Y. Yue, G. Sheng, H. Lai, S. Wang, L. Yu, Q. Zhang, F. Feng, Z. T. Hu, X. Li, Nitrogen- and phosphorus-codoped carbon-based catalyst for acetylene hydrochlorination, *J. Catal.* 373 (2019) 240–249, <https://doi.org/10.1016/j.jcat.2019.03.044>.
- [35] X. Liu, X. Qiao, Z. Zhou, C. Zhao, Q. Guan, W. Li, Mechanism exploring of acetylene hydrochlorination using hexamethylenetetramine as a single active site metal-free catalyst, *Catal. Commun.* 147 (2020), 106147, <https://doi.org/10.1016/j.catcom.2020.106147>.
- [36] X.F. Zhou, S.G. Xu, Y.L. Liu, S.K. Cao, Mechanistic study on metal-free acetylene hydrochlorination catalyzed by imidazolium-based ionic liquids, *Mol. Catal.* 461 (2018) 73–79, <https://doi.org/10.1016/j.mcat.2018.04.027>.
- [37] C.E. Yeom, M.J. Kim, B.M. Kim, 1,8-Diazabicyclo[5.4.0]undec-7-ene (DBU)-promoted efficient and versatile aza-Michael addition, *Tetrahedron* 63 (2007) 904–909, <https://doi.org/10.1016/j.tet.2006.11.037>.
- [38] A.G. Ying, R.H. Zheng, C.L. Wu, H.D. Liang, C.H. Ge, H.J. Jiang, Michael addition of methylene active compounds to chalcones with novel task-specific ionic liquids as catalysts under solvent-free conditions, *Chin. J. Org. Chem.* 31 (2011) 1312–1318.
- [39] H. Yuan, J. Zhang, [DBU-H]⁺ and H₂O as effective catalyst form for 2,3-dihydropyrido[2,3-d]pyrimidin-4(1H)-ones: a DFT study, *J. Comput. Chem.* 36 (2015) 1295–1303, <https://doi.org/10.1002/jcc.23923>.
- [40] M.J. Frisch, G.W. Trucks, H.B. Schlegel, G.E. Scuseria, M.A. Robb, J.R. Cheeseman, G. Scalmani, V. Barone, B. Mennucci, G.A. Petersson, H. Nakatsuji, M. Caricato, X. Li, H. P. Hratchian, A.F. Izmaylov, G.Z.J. Bloino, J.L. Sonnenberg, M. Hada, M. Ehara, K. Toyota, R. Fukuda, J. Hasegawa, M. Ishida, T. Nakajima, Y. Honda, O. Kitao, H. Nakai, T. Vreven, J.A. Montgomery, J.E. Peralta, F. Ogliaro, M. Bearpark, J.J. Heyd, E. Brothers, K.N. Kudin, V.N. Staroverov, T. Keith, R. Kobayashi, J. Normand, A. Rendell, J.C. Burant, S.S. Iyengar, J. Tomasi, M. Cossi, N. Rega, J.M. Millam, M. Klene, J.E. Knox, J.B. Cross, V. Bakken, C. Adamo, J. Jaramillo, R. Gomperts, R. E. Stratmann, O. Yazyev, A.J. Austin, R. Cammi, C. Pomelli, J.W. Ochterski, R. L. Martin, K. Morokuma, V.G. Zakrzewski, G.A. Voth, P. Salvador, J.J. Dannenberg, S. Dapprich, A.D. Daniels, O. Farkas, J.B. Foresman, J.V. Orti, J. Cioslowski, D. J. Fox, Gaussian 09, Revision D.01, Gaussian, Inc., Wallingford CT, 2013. ES64L-G09RevD.01 24-Apr-2013.
- [41] A.D. Becke, Density-functional thermochemistry. I. The effect of the exchange-only gradient correction, *J. Chem. Phys.* 96 (1992) 2155–2160, <https://doi.org/10.1063/1.462066>.
- [42] A.D. Becke, Density-functional thermochemistry. II. The effect of the Perdew-Wang generalized-gradient correlation correction, *J. Chem. Phys.* 97 (1992) 9173–9177, <https://doi.org/10.1063/1.463343>.
- [43] A.D. Becke, Density-functional thermochemistry. III. The role of exact exchange, *J. Chem. Phys.* 98 (1993) 5648–5652, <https://doi.org/10.1063/1.464913>.
- [44] K. Fukui, The path of chemical reactions - the IRC approach, *Acc. Chem. Res.* 14 (1981) 363–368, <https://doi.org/10.1021/ar00072a001>.
- [45] C. Gonzalez, H.B. Schlegel, Reaction path following in mass-weighted internal coordinates, *J. Phys. Chem.* 94 (1990) 5523–5527, <https://doi.org/10.1021/j100377a021>.
- [46] Z. Shen, Y. Liu, Y. Han, Y. Qin, J. Li, P. Xing, B. Jiang, Nitrogen-doped porous carbon from biomass with superior catalytic performance for acetylene hydrochlorination, *RSC Adv.* 10 (2020) 14556–14569, <https://doi.org/10.1039/D0RA00475H>.
- [47] X. Li, Y. Nian, S. Shang, H. Zhang, J. Zhang, Y. Han, W. Li, Novel nonmetal catalyst of supported tetraphenylphosphonium bromide for acetylene hydrochlorination, *Catal. Sci. Technol.* 9 (2019) 188–198, <https://doi.org/10.1039/c8cy02103a>.
- [48] X. Li, J. Zhang, Y. Han, M. Zhu, S. Shang, W. Li, MOF-derived various morphologies of N-doped carbon composites for acetylene hydrochlorination, *J. Mater. Sci.* 53 (2017) 4913–4926, <https://doi.org/10.1007/s10853-017-1951-3>.
- [49] Z. Lasemi, M. Tajbakhsh, H. Alinezhad, F. Mehrparvar, 1,8-Diazabicyclo [5.4.0] undec-7-ene functionalized cellulose nanofibers as an efficient and reusable nanocatalyst for the synthesis of tetraketones in aqueous medium, *Res. Chem. Intermed.* 46 (2020) 3667–3682, <https://doi.org/10.1007/s11164-020-04167-y>.
- [50] K. Chen, L.H. Kang, M.Y. Zhu, B. Dai, Mesoporous carbon with controllable pore sizes as a support of the AuCl₃ catalyst for acetylene hydrochlorination, *Catal. Sci. Technol.* 5 (2015) 1035–1040, <https://doi.org/10.1039/c4cy01172d>.
- [51] W. Zhao, W. Li, J.L. Zhang, Ru/N-AC catalyst to produce vinyl chloride from acetylene and 1,2-dichloroethane, *Catal. Sci. Technol.* 6 (2016) 1402–1409, <https://doi.org/10.1039/c5cy01277e>.
- [52] C.M. Zhang, H.Y. Zhang, B.C. Man, X. Li, H. Dai, J.L. Zhang, Hydrochlorination of acetylene catalyzed by activated carbon supported highly dispersed gold nanoparticles, *Appl. Catal. A* 566 (2018) 15–24, <https://doi.org/10.1016/j.apcata.2018.08.012>.
- [53] Y. Dong, W. Li, Z. Yan, J. Zhang, Hydrochlorination of acetylene catalyzed by an activated carbon supported chlorotriphenylphosphine gold complex, *Catal. Sci. Technol.* 6 (2016) 7946–7955, <https://doi.org/10.1039/c6cy01241h>.
- [54] X. Qi, W. Chen, J. Zhang, Sulphur-doped activated carbon as a metal-free catalyst for acetylene hydrochlorination, *RSC Adv.* 10 (2020) 34612–34620, <https://doi.org/10.1039/D0RA06256A>.
- [55] H. Li, B.T. Wu, F.M. Wang, X.B. Zhang, Achieving efficient and low content ru-based catalyst for acetylene hydrochlorination based on N,N'-dimethylpropyleneurea, *ChemCatChem* 10 (2018) 4090–4099, <https://doi.org/10.1002/cctc.201801000>.
- [56] C. Zhao, X. Qiao, Z. Yi, Q. Guan, W. Li, Active centre and reactivity descriptor of a green single component imidazole catalyst for acetylene hydrochlorination, *PCCP* 22 (2020) 2849–2857, <https://doi.org/10.1039/C9CP06005G>.